On the Oxidation of Ammonia and Mutual Sensitization of the Oxidation No and Ammonia: Experimental and Kinetic Modeling

Philippe Dagaut

ON THE OXIDATION OF AMMONIA AND MUTUAL SENSITIZATION OF THE OXIDATION NO AND AMMONIA: EXPERIMENTAL AND KINETIC MODELING

Philippe Dagaut*
dagaut@cnrs-orleans.fr
*CNRS–INSIS, ICARE, 1C Avenue de la recherche scientifique, 45071 Orléans, cedex2, France

Abstract
The selective non-catalytic reduction of NO by ammonia (SNCR) has been extensively studied but no activation of ammonia oxidation by nitric oxide had been reported. Experiments performed in a jet-stirred reactor (JSR) at atmospheric pressure for various equivalence ratios (0.1–2) and initial concentrations of NH_3 (500 to 1000 ppm) and NO (0 to 1000 ppm) revealed kinetic interactions similar to the so-called mutual sensitization of the oxidation of hydrocarbons and NO. The experiments were performed at fixed residence times of 100 and 200 ms, and variable temperature ranging from 1100 to 1450 K. Kinetic reaction mechanisms were used to simulate these experiments and ammonia oxidation. The most reliable model from the literature was updated (NH_2+H → NH+H_2, HNO+H → NO+H_2) to better predict ammonia-air burning velocities. It showed the mutual sensitization of the oxidation of ammonia and nitric oxide proceeds through several reaction pathways leading to OH production which is mainly responsible for ammonia oxidation in the current conditions: NH_2 + NO → NNH + OH, NNH → N_2 + H, NNH + O_2 → N_2 + HO_2, H + O_2 → OH + O, H + O_2 + M → HO_2 + M, and NO + HO_2 → NO_2 + OH.

Keywords: ammonia, kinetics, modeling, jet-stirred reactor, nitric oxide

Introduction

Thermal de-NO, also called selective non-catalytic reduction of NO by ammonia (SNCR), is a common NO reduction technique which is efficient in a small temperature range centered around 1200–1250 K. Many experimental and kinetic modeling studies concern SNCR (Dagaut and Nicolle 2005a; Javed *et al.* 2008; Miller and Bowman 1989; Miller and Glarborg 1999; Schmidt and Bowman 2001). However, existing kinetic models show weaknesses and sometimes fail to represent the kinetics of ammonia oxidation (Kobayashi *et al.* 2019) whereas interest for this fuel or energy carrier is growing. Nowadays, ammonia is viewed as an alternative zero-carbon fuel which presents potential for future power stations (Kobayashi *et al.* 2019). In this context, ammonia combustion in a gas turbine was recently demonstrated in Japan (Kurata *et al.* 2017). However, its combustion needs further studies (Kobayashi *et al.* 2019) and kinetic interpretation needs further investigations. Therefore, experiments were performed in a JSR at atmospheric pressure for various equivalence ratios (0.1–2), for several initial concentrations of NH_3 and NO, at fixed residence times and variable temperature. Kinetic modeling was used to interpret the results and delineate reaction pathways.

Experimental

The experiments were performed in a fused-silica JSR presented earlier (Dagaut *et al.* 1986; Le Cong *et al.* 2008). A 40 mm o.d. spherical sphere (27.5 cm^3 internal volume) equipped with 4 injectors having nozzles of 1 mm i.d., for the admission of the gases achieving the stirring, constitutes the JSR. It is located inside a temperature controlled oven of c.a.1.5 kW, surrounded by insulating material; it operates at atmospheric pressure. The experiments were performed at high nitrogen dilution. Ammonia, NO, N_2, and O_2 flow rates were measured and regulated by thermal mass-flow controllers. The reactor operated under macro-mixing conditions, allowing the use of a perfectly-stirred reactor model. The mixing time was ca. 70 times shorter than the residence time in the reactor. A good thermal homogeneity along the whole vertical axis of the reactor was obtained in the experiments. The temperature was measured using a Pt/Pt-Rh10% thermocouple of 0.1 mm diameter located inside a thin-wall fused-silica tube (<0.5mm), which prevents catalytic reactions on the metal wires. The high degree of dilution used in these experiments yielded a small temperature rise in the JSR (<20 K). Typical temperature variations of < 8 K along the vertical axis of the JSR were measured. Low pressure samples of the reacting mixture (30–40 Torr) were taken using a sonic quartz probe, for immediate multi-dimensional gas chromatography (GC) analyses. In order to improve the GC detection, these samples were pressurized at 1 bar before injection into the GC column, using a home-made glass piston. A thermal conductivity detector was used for quantifying permanent gases and on-line Fourier transform infrared (FTIR) was used for measuring H_2O, NO, NO_2, N_2O, and NH_3.The uncertainties on mole fractions were ±10% for the reactants and products. For NO_2, formed at trace concentrations, the uncertainty was ±2 ppm based on FTIR analysis. Uncertainties in reactant mole fractions are typically <10%, in residence time <5%, in pressure <0.1 atmosphere, and ±4 K for temperature.

Modeling

The computations were performed using the PSR computer code (Glarborg *et al.* 1986), which computes species concentrations from the balance between the net rate of production of each species by chemical reactions, and the difference between the input and output flow rates of species.

Several literature kinetic reaction mechanisms were used. We used our previously published SNCR-SO_x mechanism (Dagaut and Nicolle 2005a), our HCN-NOx mechanism called DGA mechanism (Dagaut *et al.* 2008), Konnov mechanism (Konnov 2009) and the ammonia mechanisms proposed by Song et al. recently (Song *et al.* 2016), and Otomo et al. (Otomo *et al.* 2018). The rate constants for the reverse reactions were computed from the forward rate constants and the equilibrium constants, using the appropriate thermochemical data.

Results and Discussion

Experiments were performed at atmospheric pressure for various equivalence ratios (0.1, 0.5, 1, and 2 with $\varphi = (NH_3\% / O_2\%) / (NH_3\% / O_2\%)_{at\ \varphi=1}$ and $NH_3 + 1.25\ O_2 \rightarrow NO + 1.5\ H_2O$), for two initial concentrations of NH_3 (500 and 1000 ppm) and several initial concentrations of NO (0, 500, and 1000 ppm).

The experiments were performed at fixed residence times τ=100 and τ=200 ms, and the temperature was varied stepwise over the range 1100 –1450 K. The mole fractions of O_2, NH_3, NO, NO_2, N_2O, and H_2O were measured. The experimental results revealed a strong influence of NO on ammonia conversion which had not been reported previously. As can be seen from Figure 1, the presence of 500–1000 ppm of NO shifts ammonia ignition by ca.-120 K in fuel-lean and fuel-rich conditions. This kinetic interaction between NO and NH_3 looks similar to mutual oxidation sensitization of hydrocarbons and NO where NO boosts the oxidation of the fuel which in turn favors the NO to NO_2 conversion (Bromly *et al.* 1996; Dagaut *et al.* 1999; Dagaut *et al.* 2001; Dagaut and Nicolle 2005b, 2005c; Dagaut *et al.* 2005; Dagaut and Dayma 2006; Dayma *et al.* 2007; Konnov *et al.* 2005; Sivaramakrishnan *et al.* 2007). The data also show that the reduction of NO by ammonia is maximized around 1250K, as already shown in the literature.

In our previous modeling of the kinetics of SNCR in a JSR (Dagaut and Nicolle 2005a), it was noted that although the kinetic model used (Skreiberg *et al.* 2004) could predict NO-reduction, the conversion of ammonia vs. temperature was too fast. Therefore, other more recent kinetic models available from the literature were tested against our JSR data (Figure 2).

As can be seen from Figure 2, the fastest oxidation of ammonia was predicted by the model of Konnov, which is consistent with observations in recent modeling efforts (Kobayashi *et al.* 2019; Nakamura and Hasegawa 2017). The most recent model of Song et al. also predicts ammonia oxidation too fast as well as that of Otomo et al. (Otomo *et al.* 2018). Therefore, the previously proposed DGA model (Dagaut *et al.* 2008) was also tested (Fig. 2c) since it was recently demonstrated by Kobayashi et al. (Figure 22) (Kobayashi *et al.* 2019) to predict well ammonia ignition measured in a shock-tube by Mathieu and Petersen (Mathieu and Petersen 2015) and ammonia burning velocities. The present modeling show that DGA model performs better than the other mechanisms tested here. However, the DGA model tends to slightly over predict ammonia-air burning velocities. Therefore, sensitivity analyses were performed in order to improve burning velocities predictions while keeping good predictions under JSR conditions. The sensitivity analyses show that the kinetics of the reactions $NH_2 + H \rightarrow NH + H_2$ and $HNO + H \rightarrow NO + H_2$ were much influencing burning velocities predictions but not JSR or shock-tube simulations. Their rate constants were updated using the kinetics proposed by Otomo et al. (Otomo *et al.* 2018). The resulting model performed rather well under flame conditions (Fig. 3).

Sensitivity analyses were performed to identify the most influential reactions in literature mechanisms and try to explain observed discrepancies between modeling and data under JSR conditions. Table 1 summarizes the results of sensitivity analyses and of reaction pathways analyses. One can see that for the four mechanisms considered, the oxidation of ammonia proceeds by H-atom abstraction by OH (83.1 to 87.4%) and to a much lesser extent, with O-atoms (12.5 to 15.7%). The importance of the reaction with H-atoms is negligible, as expected under fuel-lean conditions. The most sensitive reactions are indicated in bold in the Table. One can notice some differences in terms of sensitivity for ammonia concentrations. It is interesting to note that the fastest mechanism (Konnov 2009), shows higher sensitivity coefficients for reactions $2\ NH_2 \leftrightarrows N_2H_2+H_2$, $N_2H_2 + M \leftrightarrows NNH + H + M$, and $NH_3 + O \leftrightarrows NH_2 + O$. These reactions have negative coefficients, indicating they can cause faster fuel consumption. Conversely, the sensitivity coefficient for the termination reaction $NH_2 + NO \leftrightarrows N_2 + H_2O$ is half what was computed with the other mechanisms. Reaction pathways analyses in the conditions of Figure 2 indicated that ammonia mostly reacts with OH radicals in the reaction mechanisms considered. At 20% fuel conversion, the formation of OH results from a limited number of reactions: $H + O_2 \leftrightarrows OH + O$, $NH_3 + O \leftrightarrows NH_2 + OH$, $NH_2 + HO_2 \leftrightarrows H_2NO + OH$, $NH_2 + NO \leftrightarrows NNH + OH$. The formation of H is dominated by the decomposition of NNH. These analyses indicate that the total rate of production of OH, H, and NNH differs significantly from one mechanism to another (Table 2). The fastest mechanism shows the highest rates of production of these active species whereas the slowest mechanism has much lower rates of production.

Figures 4–7 present comparisons between the experimental results obtained for the oxidation of neat ammonia from fuel-lean to fuel-rich conditions. They show that the updated DGA mechanism predicts well the oxidation of the fuel whereas, for minor products, the agreement between the modeling and the experiments could be improved.

The model was also tested for the NO-seeded experiments from fuel-lean to fuel rich conditions for which enhanced ammonia oxidation rate by NO was observed. The results are presented in Figures 8–10 where the good predictions of the updated DGA model are demonstrated.

Reaction pathway analyses were performed to delineate the mechanism responsible for the mutual sensitization of ammonia and nitric oxide. In the conditions of Figure 4 (1000 ppm of NH_3, τ=100ms; φ=0.1) and Figure 8 (1000 ppm of NH_3 and 500 ppm of NO, τ=100ms; φ=0.1). Schematic presentations are given in Figures 11a and 11b, respectively. The analyses were performed at 1197 K corresponding to the temperature at which ammonia starts to react.

The neat oxidation of ammonia mainly proceeds through oxidation by OH (78%) and O (21%), yielding the NH_2 radical. This radical oxidizes by reaction with HO_2 (45%) and O_2 (12%), yielding H_2NO. H_2NO oxidizes by reaction with O_2 (48%) yielding HO_2 and HNO, and by reaction with NH_2 also yielding HNO. HNO oxidizes by reaction with O_2 yielding HO_2 and NO which in turn is reduced by reaction with NH_2. The decomposition of NNH, formed by the reaction of NO and NH_2, yields H atoms which provide branching through reaction with O_2: $H+O_2 \rightarrow OH+O$.

When 500 ppm of NO are introduced, ammonia is still mainly oxidized by OH (87%) and O (12%), yielding the NH_2 radical. This radical still oxidizes by reaction with HO_2, but to a much less extent (<2%). The NH_2 radical mostly reacts with NO to form N_2 (57%) and NNH (34%). The decomposition of NNH, yields H atoms (67%), which provide branching through reaction with O_2: $H+O_2 \rightarrow OH+O$, and HO_2 by reaction with O_2 (26%). NO reaction with HO_2 (13%) also contributes to OH production (16%).

Figure 12 shows the evolution of the importance of the main reactions consuming NO. One can see that the importance of reaction 165, responsible for NO_2 formation, is decreasing with increasing temperature. At low temperature, it is the third most important reaction pathway while at 1500 K it becomes one of the less important.

Conclusion

Experiments performed in a jet-stirred reactor (JSR) at atmospheric pressure for various equivalence ratios (0.1–2) and initial concentrations of NH_3 (500 to 1000 ppm) and NO (0 to 1000 ppm) revealed kinetic interactions between ammonia and nitric oxide similar to the mutual sensitization of the oxidation of hydrocarbons and NO. The experiments were performed at fixed residence times of 100 and 200 ms, and variable temperature, ranging from 1100 to 1450 K. An existing model (Dagaut *et al.* 2008) was updated to improve the modeling of ammonia-air flame speed. It was used to simulate the JSR experiments and ammonia ignition and burning velocities. According to that model, the mutual sensitization of the oxidation of ammonia and nitric oxide proceeds through reaction pathways leading to OH production, mainly responsible for the oxidation of ammonia. In the JSR conditions, the production of OH radicals results from a sequence of reaction including: $NH_2 + NO \rightarrow NNH + OH$, $NNH \rightarrow N_2 + H$, $H + O_2 \rightarrow OH + O$, and $NO + HO_2 \rightarrow NO_2 + OH$. The HO_2 radical is mainly produced via: $NNH + O_2 \rightarrow N_2 + HO_2$ and $H + O_2 + M \rightarrow HO_2 + M$.

References

Bromly, J.H., Barnes, F.J., Muris, S., You, X., and Haynes, B.S. (1996) Kinetic and thermodynamic sensitivity analysis of the NO-sensitised oxidation of methane. *Combust Sci Technol,* 115, 259-96.

Dagaut, P. and Nicolle, A. (2005a) Experimental and kinetic modeling study of the effect of SO2 on the reduction of NO by ammonia. *Proceedings of the Combustion Institute,* 30 (1), 1211-18.

Dagaut, P. and Nicolle, A. (2005b) Experimental and kinetic modeling study of the effect of sulfur dioxide on the mutual sensitization of the oxide and methane. *International Journal of Chemical Kinetics,* 37 (7), 406-13.

Dagaut, P. and Nicolle, A. (2005c) Experimental study and detailed kinetic modeling of the effect of exhaust gas on fuel combustion: mutual sensitization of the oxidation of nitric oxide and methane over extended temperature and pressure ranges. *Combustion and Flame,* 140 (3), 161-71.

Dagaut, P. and Dayma, G. (2006) Mutual Sensitization of the oxidation of nitric oxide and a natural gas blend in a JSR at elevated pressure: Experimental and detailed kinetic modeling study. *Journal of Physical Chemistry a,* 110 (21), 6608-16.

Dagaut, P., Luche, J., and Cathonnet, M. (2001) The low temperature oxidation of DME and mutual sensitization of the oxidation of DME and nitric oxide: Experimental and detailed kinetic modeling. *Combustion Science and Technology,* 165, 61-84.

Dagaut, P., Glarborg, P., and Alzueta, M.U. (2008) The oxidation of hydrogen cyanide and related chemistry. *Progress in Energy and Combustion Science,* 34 (1), 1-46.

Dagaut, P., Lecomte, F., Chevailler, S., and Cathonnet, N. (1999) Mutual sensitization of the oxidation of nitric oxide and simple fuels over an extended temperature range: Experimental and detailed kinetic modeling. *Combustion Science and Technology,* 148 (1-6), 27-57.

Dagaut, P., Mathieu, O., Nicolle, A., and Dayma, G. (2005) Experimental study and detailed kinetic modeling of the mutual sensitization of the oxidation of nitric oxide, ethylene, and ethane. *Combustion Science and Technology,* 177 (9), 1767-91.

Dagaut, P., Cathonnet, M., Rouan, J.P., Foulatier, R., Quilgars, A., Boettner, J.C., Gaillard, F., and James, H. (1986) A Jet-Stirred Reactor for Kinetic-Studies of Homogeneous Gas-Phase Reactions at Pressures up to 10-Atmospheres (~ 1 MPa). *Journal of Physics E-Scientific Instruments,* 19 (3), 207-09.

Dayma, G., Hadj Ali, K., and Dagaut, P. (2007) Experimental and detailed kinetic modeling study of the high pressure oxidation of methanol sensitized by nitric oxide and nitrogen dioxide. *Proceedings of the Combustion Institute,* 31 (1), 411-18.

Glarborg, P., Kee, R.J., Grcar, J.F., and Miller, J.A. (1986). PSR: A FORTRAN program for modeling well-stirred reactors. SAND86-8209, *SAND86-8209* (Livermore, CA: Sandia National Laboratories).

Hayakawa, A., Goto, T., Mimoto, R., Arakawa, Y., Kudo, T., and Kobayashi, H. (2015) Laminar burning velocity and Markstein length of ammonia/air premixed flames at various pressures. *Fuel,* 159, 98-106.

Javed, M.T., Ahmed, Z., Ibrahim, M.A., and Irfan, N. (2008) A comparative kinetic study of SNCR process using ammonia. *Brazilian Journal of Chemical Engineering,* 25 (1), 109-17.

Kobayashi, H., Hayakawa, A., Somarathne, K.D.Kunkuma A., and Okafor, Ekenechukwu C. (2019) Science and technology of ammonia combustion. *Proceedings of the Combustion Institute,* 37 (1), 109-33.

Konnov, A.A. (2009) Implementation of the NCN pathway of prompt-NO formation in the detailed reaction mechanism. *Combustion and Flame,* 156 (11), 2093-105.

Konnov, A.A., Barnes, F.J., Bromly, J.H., Zhu, J.N., and Zhang, D.K. (2005) The pseudo-catalytic promotion of nitric oxide oxidation by ethane at low temperatures. *Combustion and Flame,* 141 (3), 191-99.

Kurata, O., Iki, N., Matsunuma, T., Inoue, T., Tsujimura, T., Furutani, H., Kobayashi, H., and Hayakawa, A. (2017) Performances and emission characteristics of NH3–air and NH3CH4–air combustion gas-turbine power generations. *Proceedings of the Combustion Institute,* 36 (3), 3351-59.

Le Cong, T., Dagaut, P., and Dayma, G. (2008) Oxidation of Natural Gas, Natural Gas/Syngas Mixtures, and Effect of Burnt Gas Recirculation: Experimental and Detailed Kinetic Modeling. *Journal of Engineering for Gas Turbines and Power,* 130 (4), 041502-10.

Mathieu, O. and Petersen, E.L. (2015) Experimental and modeling study on the high-temperature oxidation of Ammonia and related NOx chemistry. *Combustion and Flame,* 162 (3), 554-70.

Mei, B., Zhang, X., Ma, S., and Li, Y. (2019). Investigation on laminar flame propagation of ammonia under oxygen enrichment and elevated pressure conditions, *12th Asia-Pacific Conference on Combustion* (Fukuoka, Japan).

Miller, J.A. and Bowman, C.T. (1989) Mechanism and modeling of nitrogen chemistry in combustion. *Progress in Energy and Combustion Science,* 15 (4), 287-338.

Miller, J.A. and Glarborg, P. (1999) Modeling the Thermal De-NOx Process: Closing in on a final solution. *International Journal of Chemical Kinetics,* 31 (11), 757-65.

Nakamura, H. and Hasegawa, S. (2017) Combustion and ignition characteristics of ammonia/air mixtures in a micro flow reactor with a controlled temperature profile. *Proceedings of the Combustion Institute,* 36 (3), 4217-26.

Otomo, J., Koshi, M., Mitsumori, T., Iwasaki, H., and Yamada, K. (2018) Chemical kinetic modeling of ammonia oxidation with improved reaction mechanism for ammonia/air and

ammonia/hydrogen/air combustion. *International Journal of Hydrogen Energy,* 43 (5), 3004-14.
Pfahl, U.J., Ross, M.C., Shepherd, J.E., Pasamehmetoglu, K.O., and Unal, C. (2000) Flammability limits, ignition energy, and flame speeds in H2–CH4–NH3–N2O–O2–N2 mixtures. *Combustion and Flame,* 123 (1), 140-58.
Ronney, P.D. (1988) Effect of Chemistry and Transport Properties on Near-Limit Flames at Microgravity. *Combustion Science and Technology,* 59 (1-3), 123-41.
Schmidt, C.C. and Bowman, C.T. (2001) Flow reactor study of the effect of pressure on the thermal De-NOx process. *Combustion and Flame,* 127 (1-2), 1958-70.
Sivaramakrishnan, R., Brezinsky, K., Dayma, G., and Dagaut, P. (2007) High pressure effects on the mutual sensitization of the oxidation of NO and CH4-C2H6 blends. *Physical Chemistry Chemical Physics,* 9 (31), 4230-44.
Skreiberg, Ø., Kilpinen, P., and Glarborg, P. (2004) Ammonia chemistry below 1400 K under fuel-rich conditions in a flow reactor. *Combustion and Flame,* 136 (4), 501-18.
Song, Y., Hashemi, H., Christensen, J.M., Zou, C., Marshall, P., and Glarborg, P. (2016) Ammonia oxidation at high pressure and intermediate temperatures. *Fuel,* 181, 358-65.
Takizawa, K., Takahashi, A., Tokuhashi, K., Kondo, S., and Sekiya, A. (2008) Burning velocity measurements of nitrogen-containing compounds. *Journal of Hazardous Materials,* 155 (1), 144-52.

TABLES

Table 1. Sensitivity and reaction pathway for ca. 25% NH_3 consumption in the conditions of Figure 2.

Reaction	Normalized sensitivity coefficients for NH3			
	Song et al.	Konnov	Otomo et al.	DGA updated
$H+O_2=O+OH$	**-0.48**	**-1.00**	**-0.42**	**-0.23**
$NH_2+O=HNO+H$	**-0.21**	**+0.32**	**-0.22**	-0.07
$NH_2+HO_2=HNO+H_2O$	+0.15	-	+0.19	+0.17
$NH_2+NO=N_2+H_2O$	**+0.93**	+0.44	**+0.97**	**+0.91**
$NH_2+NO=NNH+OH$	**-0.52**	**-0.51**	**-1.00**	**-1.00**
$H+O_2+M=HO_2+M$	**-1. 00**	**+0.66**	+0.10	-0.05
$2NH_2=N_2H_2+H_2$	+0.02	**-0.83**	-	-
$N_2H_2+M=NNH+H+M$	-0.08	**-0.73**	-0.08	-
$NH_3+O=NH_2+OH$	+0.05	**-0.74**	+0.09	-0.04
$NH+O_2=HNO+O$	-0.06	-	-0.10	-0.17
$H_2NO+O_2=HNO+HO_2$	-0.07	-	-0.13	-0.20
$H_2NO+NH_2=HNO+NH_3$	+0.05	+0.13	+0.08	+0.17
$HNO+O_2=HO_2+NO$	**+0.26**	-	**+0.34**	+0.16
$H+NO+M=HNO+M$	**-0.32**	-0.07	**-0.38**	-0.20
	% NH_3 consumption			
$NH_3+OH=NH_2+H_2O$	**85.7**	**87.4**	**83.1**	**85.3**
$NH_3+O=NH_2+OH$	**13.6**	**12.5**	**15.7**	**14.2**
$NH_3+H=HN_2+H_2$	**-**	**-**	**1.2**	**-**

Table 2. Reaction pathways analysis at 20% ammonia conversion in a JSR (1000 ppm of NH_3, 12500 ppm of O_2, τ=100ms; φ=0.1). Rates are given in mole, cm^{-3}, s^{-1} units.

Species	(Konnov 2009)	(Song *et al.* 2016)	(Otomo *et al.* 2018)	Updated DGA
OH	2.60E-8	2.30E-8	2.05E-8	2.05E-8
H	1.59E-8	7.68E-9	6.72E-9	3.97E-9
NNH	7.65E-9	3.57E-9	2.68E-9	3.02E-9

FIGURES

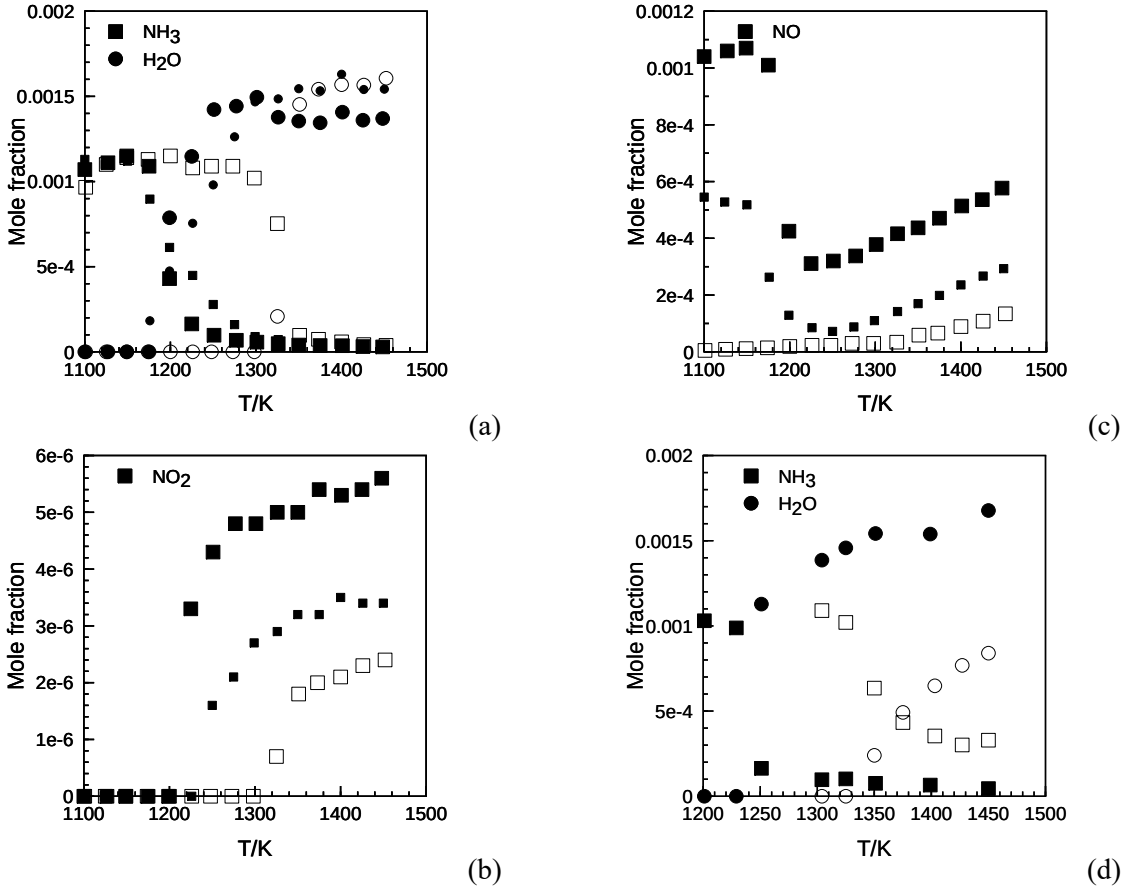

Figure 1. Impact of the initial concentration of NO on NH_3 conversion. Experimental results obtained in a JSR at 1 bar. (a–c): 1000 ppm NH_3, 12500 ppm of O_2, τ=100ms; φ=0.1; 0 (open symbols), 500 (small black symbols), 1000 (large black symbols) ppm NO; (d): 1000 ppm NH_3, 625 ppm of O_2, 200ms; φ=2; 0(open symbols), and 1000 (large black symbols) ppm NO.

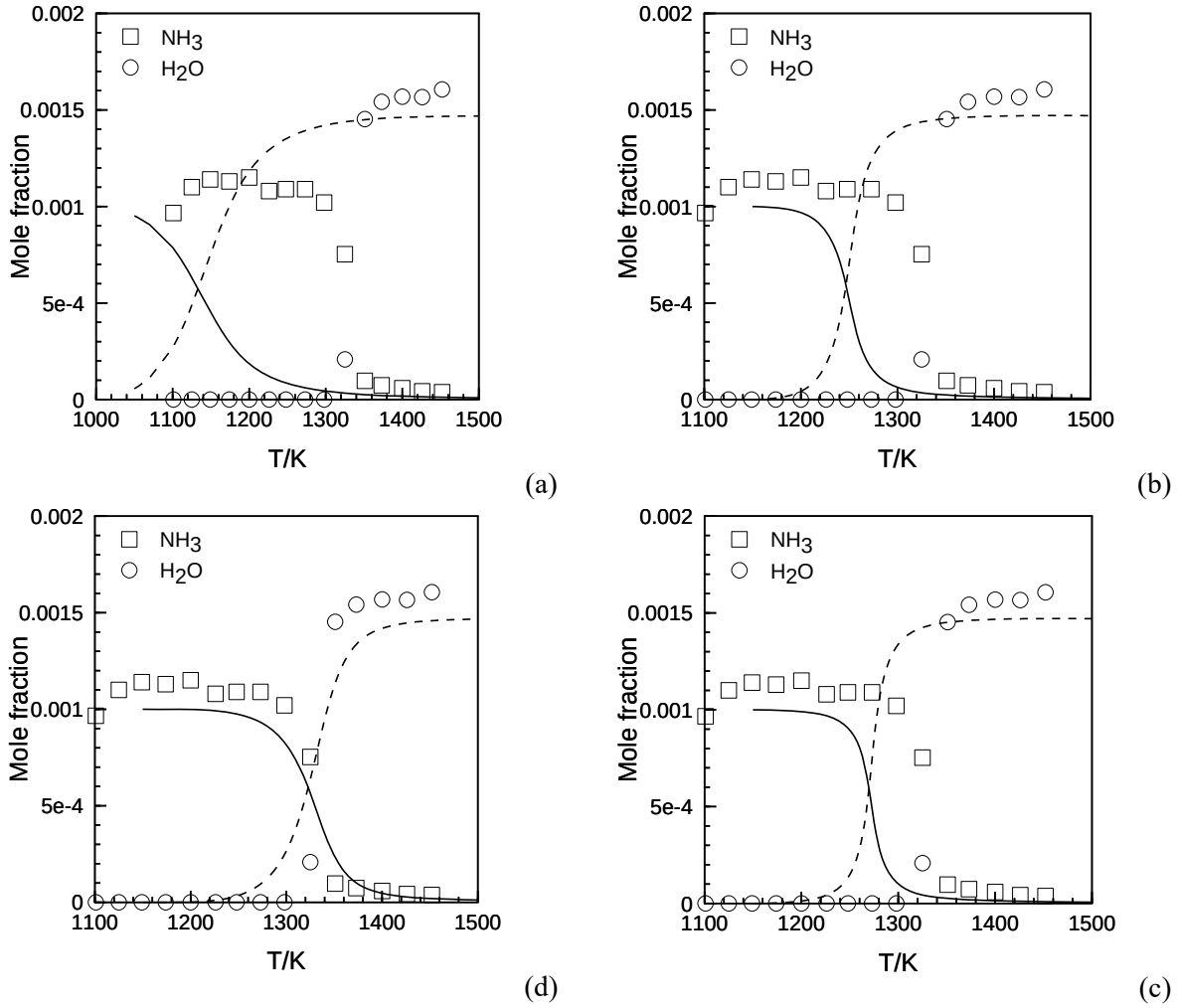

Figure 2. Comparison between experimental (symbols) and computed (lines) results for the oxidation of NH_3 in a JSR: 1000 ppm of NH_3, 12500 ppm of O_2, τ=100ms; φ=0.1. Literature models: (a) Konnov (Konnov 2009), (b) Song et al.(Song *et al.* 2016), (c) Otomo et al. (Otomo *et al.* 2018) , (d) Dagaut et al. (Dagaut *et al.* 2008).

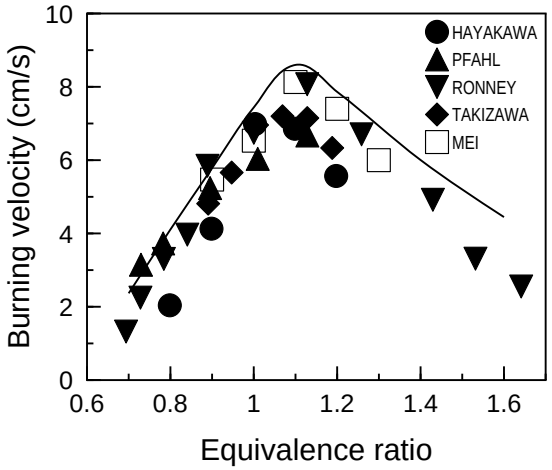

Figure 3. Computed (lines) and experimental (symbols) results for NH_3-air flames at 1 atm. The data were taken from the literature (Hayakawa *et al.* 2015; Mei *et al.* 2019; Pfahl *et al.* 2000; Ronney 1988; Takizawa *et al.* 2008). Uncertainties are estimated not to be less that 2 cm/s. Equivalence ratios based on $4\ NH_3 + 3\ O_2 \rightarrow 2\ N_2 + 6\ H_2O$.

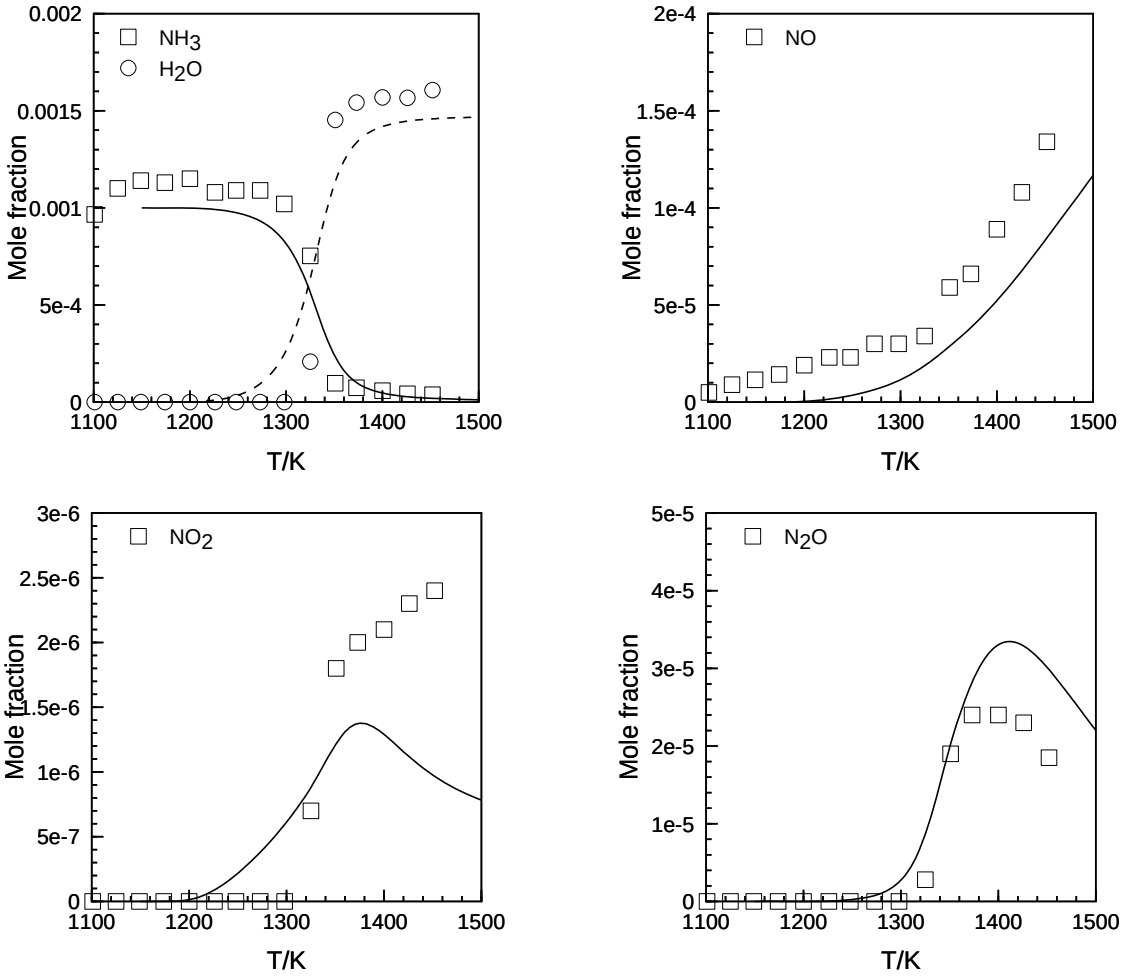

Figure 4. Comparison between experimental (symbols) and computed (lines) results for the oxidation of NH_3 in a JSR: 1000 ppm of NH_3, 12500 ppm of O_2, τ=100ms; φ=0.1.

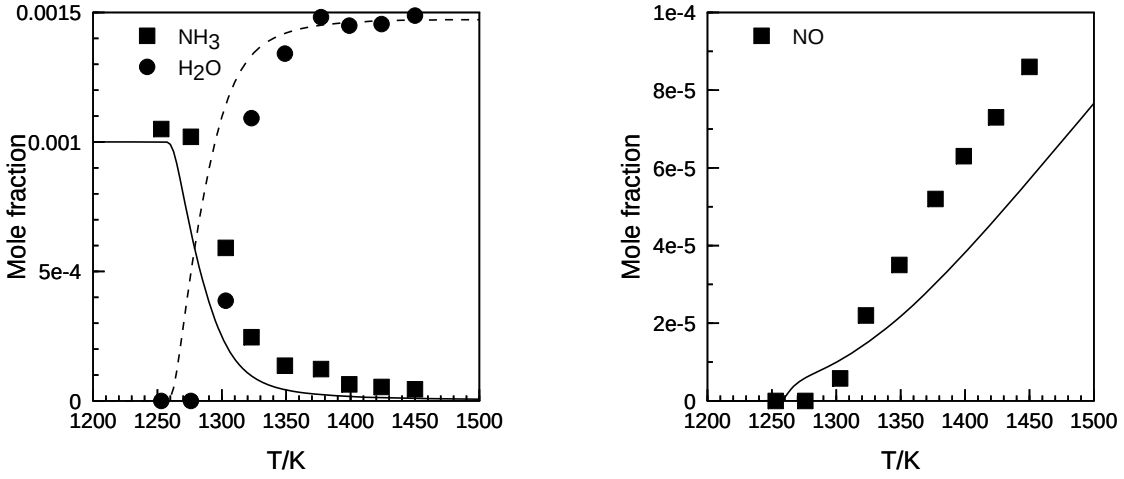

Figure 5. Comparison between experimental (symbols) and computed (lines) results for the oxidation of NH_3 in a JSR: 1000 ppm of NH_3, 2500 ppm of O_2, τ=200ms; φ=0.5.

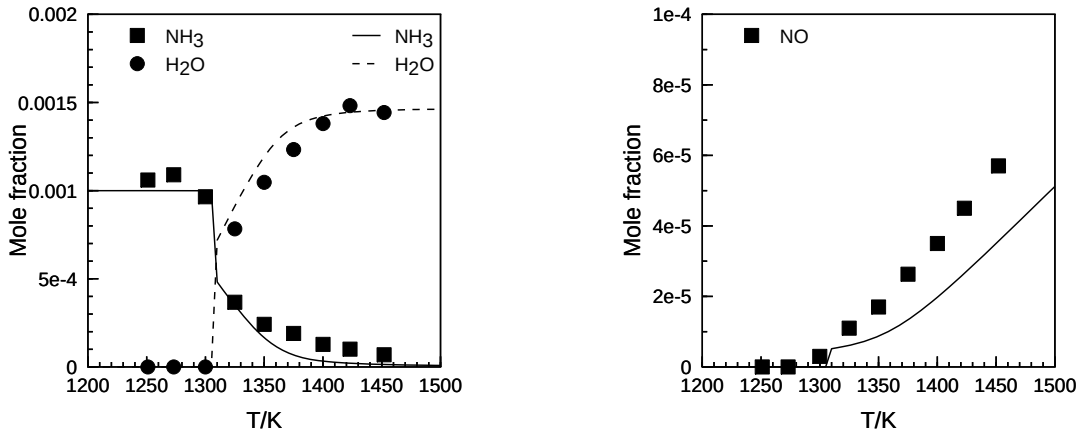

Figure 6. Comparison between experimental (symbols) and computed (lines) results for the oxidation of NH_3 in a JSR: 1000 ppm of NH_3, 1250 ppm of O_2, τ=200ms; φ=1

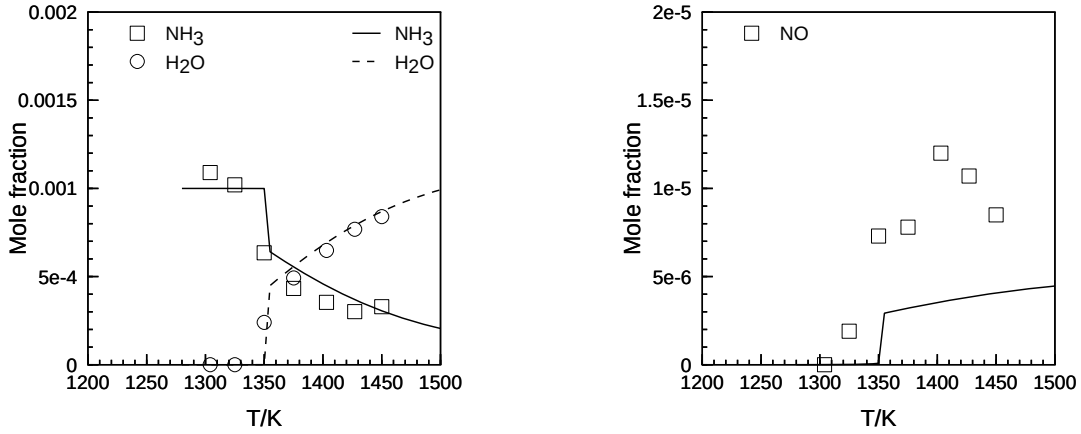

Figure 7. Comparison between experimental (symbols) and computed (lines) results for the oxidation of NH_3 in a JSR: 1000 ppm of NH_3, 625 ppm of O_2, τ=200ms; φ=2.

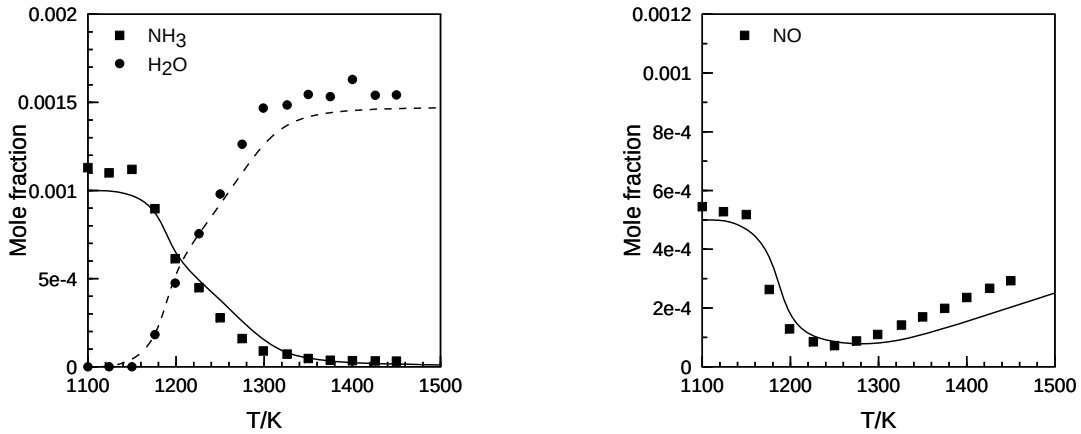

Figure 8. Comparison between experimental (symbols) and computed (lines) results for the oxidation of NH_3 in a JSR: 1000 ppm of NH_3, 12500 ppm of O_2, and 500 ppm of NO, τ=100ms; φ=0.1.

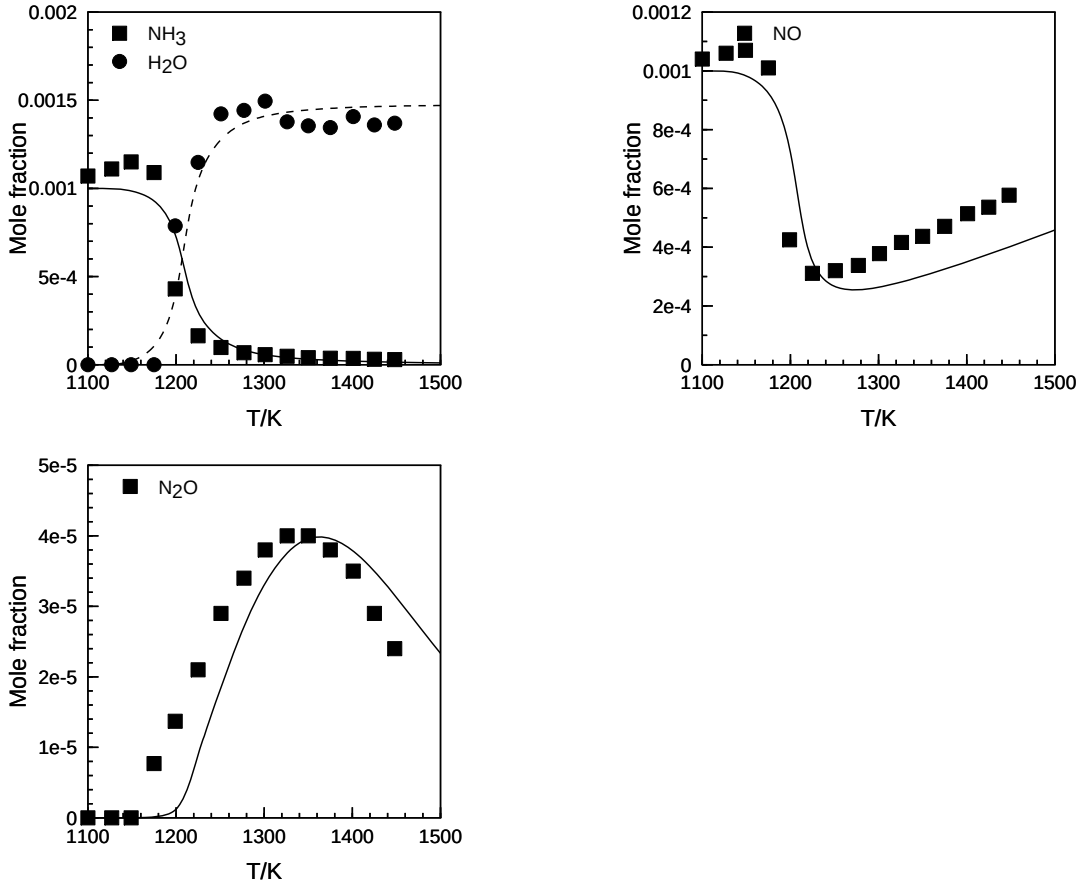

Figure 9. Comparison between experimental (symbols) and computed (lines) results for the oxidation of NH_3 in a JSR: 1000 ppm of NH_3, 12500 ppm of O_2, and 1000 ppm of NO, τ=100ms; φ=0.1.

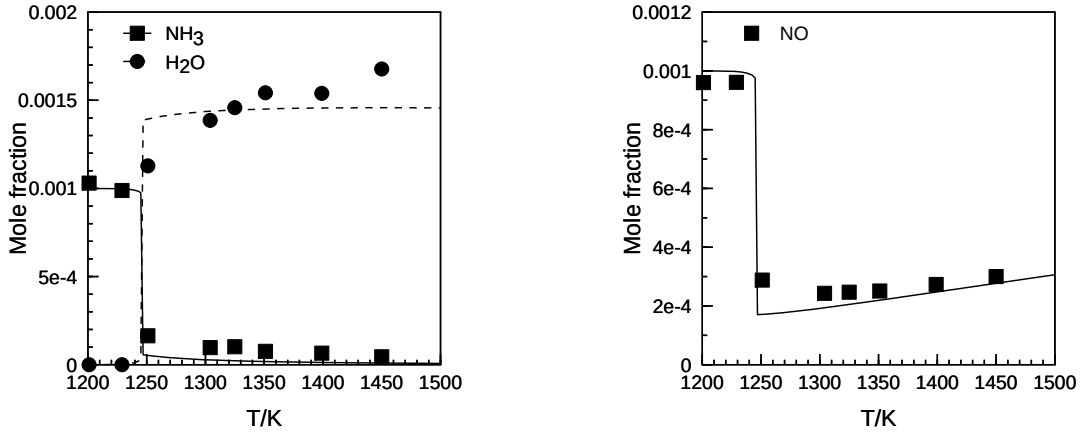

Figure 10. Comparison between experimental (symbols) and computed (lines) results for the oxidation of NH_3 in a JSR: 1000 ppm of NH_3, 625 ppm of O_2, and 1000 ppm of NO, τ=200ms; φ=2.

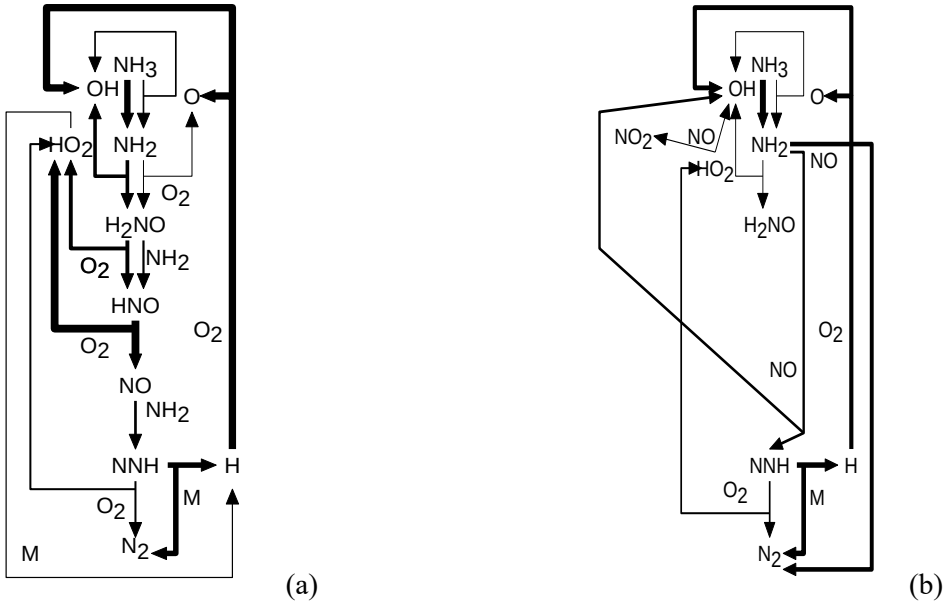

Figure 11. Computed reaction pathways for the oxidation of NH_3 in a JSR using the updated DGA model. (a): 1000 ppm of NH_3, 12500 ppm of O_2, τ=100ms; φ=0.1; (b): 1000 ppm of NH_3 and 500 ppm of NO, τ=100ms; φ=0.1.

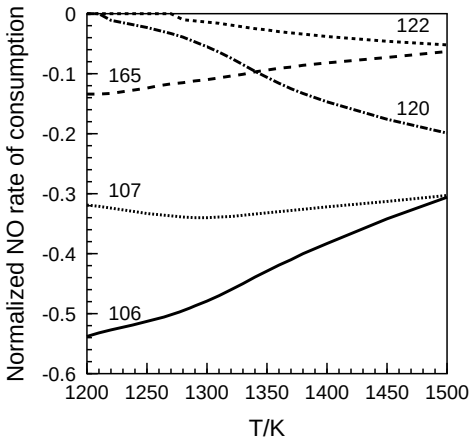

Figure 12. Computed reaction pathways for the conversion of NO in a JSR using the updated DGA model (1000 ppm of NH_3, 12500 ppm of O_2, and 500 ppm of NO, τ=100ms; φ=0.1). Important reactions are 106: $NH_2 + NO \leftrightarrows N_2 + H_2O$; 107: $NH_2 + NO \leftrightarrows NNH + OH$; 120: $NH + NO \leftrightarrows N_2O + H$; 122: $NH + NO \leftrightarrows N_2 + OH$; 165: $NO + HO_2 \leftrightarrows NO_2 + OH$.